Significant differences between nuclear-spin relaxation and conductivity relaxation in low-conductivity glasses

O. Kanert and R. Küchler
Institute of Physics, University of Dortmund, D-44221 Dortmund, Germany

K. L. Ngai
Naval Research Laboratory, Washington, D.C. 20375

H. Jain
Department of Materials Science and Engineering, Lehigh University, Bethlehem, Pennsylvania 18015
(Received 25 June 1993)

A unified model of ionic motion in glasses is presented which relates consistently the different quantities observed in nuclear-spin relaxation and electrical-conductivity relaxation due to thermally activated ionic diffusion. Corresponding experimental data obtained in a low-ionic-conductivity fluorozirconate glass are shown to be in reasonable agreement with the present approach. Limitations of the model are pointed out and are discussed in view of observed deviations between the different experimental results.

I. INTRODUCTION

The diffusive ion motion in vitreous ionic conductors can be studied either by electrical-conductivity relaxation (ECR) or by spin-lattice relaxation (SLR) in nuclear magnetic resonance (NMR). In SLR measurements can be made using either the mobile ion nucleus or an immobile nucleus permanently tied to the glassy matrix structure. Although both ECR and SLR monitor the ion motion, *a priori* it is not clear whether the ion relaxation characteristics (e.g., time scale of relaxation, activation energy, and nonexponentiality parameter) deduced from the two probes are the same or not. To answer this question, we have been performing ECR and SLR measurements on the same ionic conductor. The first series of measurements were on the alkali oxide glasses.[1] Usually the slow mobility of alkali ions in the oxide glasses does not permit observation of a maximum in the SLR rate, $1/T_1$, at temperatures below the glass transition temperature, T_g. The $1/T_1$ maximum is defined by the condition $\omega\tau_s \simeq 1$. However, for typical Larmor frequencies ω (typically 10–100 MHz) the ionic motion-induced spin correlation time τ_s is larger than $1/\omega$ in the entire temperature range, i.e., $\omega\tau_s > 1$. Thus, a determination of τ_s is not available from $1/T_1$ data, and a comparison cannot be made with the corresponding conductivity correlation time, τ_σ, obtainable from dielectric measurements carried out in a much lower frequency region (typically $10 < \omega/2\pi < 10^6$ Hz). Nevertheless, we can compare the activation energy, E_s^l of $1/T_1$ in the low-temperature regime ($\omega\tau_s \gg 1$), with the dc-conductivity activation energy $E_\sigma^{\rm dc}$ and the ac-conductivity activation energy $\bar{E}(\omega\tau_\sigma \ll 1)$. From experimental studies of many alkali oxide glasses[1] and fluorozirconate glasses,[2,3] we have established the relation

$$E_s^l = (1-n_\sigma)E_\sigma^{\rm dc} = \bar{E} \tag{1}$$

between E_s^l and $E_\sigma^{\rm dc}$ by means of a coupling coefficient n_σ with $0 \lesssim n_\sigma \lesssim 1$. For these low-conductivity ionic conductors, we recognized that the only way to obtain the SLR rate maximum, i.e., to measure the correlation time τ_s, is to go into the rotating frame and measure $1/T_{1\rho}$ at a lower frequency in the kHz range. We have implemented this idea by performing $1/T_1$ and $1/T_{1\rho}$ measurements in a number of fluorozirconate glasses.[2–4] As shown in detail in Sec. IV, one observes a significant difference between τ_s and τ_σ. Generally, in the relevant temperature region one obtains $\tau_s \gg \tau_\sigma$ due to different activation energies and preexponential times. In this context we refer to a recent work by Tatsumisago, Angell, and Martin[5] in which they have found the same difference between τ_s and τ_σ in superionic conductors including a $(LiCl)_{0.6}$-$(Li_2O)_{0.7}$-$(B_2O_3)_{1.0}$ glass. As the ionic mobility is extremely high in these superionic glasses, the laboratory frame SLR rate, $1/T_1$, shows a maximum below T_g without having to go to the rotating frame. They found the conductivity correlation at 500 K occurs on a time scale shorter by 2 orders of magnitude than the ^{7}Li SLR correlation, alike to what we have found in fluorozirconate glasses by means of rotating frame SLR measurements. Similar results were recently obtained by Munro, Schrader, and Heitjans in fast ionic-conducting lithium aluminosilicate glasses by comparing T_1 and conductivity data.[6] It is the aim of the present paper to interpret the observed differences between the two correlation times τ_σ and τ_s in the frame of a unified model relating SLR and ECR in a simplified manner. The model is based on the results of recent Monte Carlo simulations of ionic motion in disordered systems performed by Meyer, Maass, and Bunde[7] and relations of the coupling model as developed by Ngai.[8–10] The unified model predicts additional relations between the different activation energies than Eq. (1) and between crossover temperatures T_s and T_σ as observed in SLR and ECR experiments (see Fig. 1).

0163-1829/94/49(1)/76(7)/$06.00

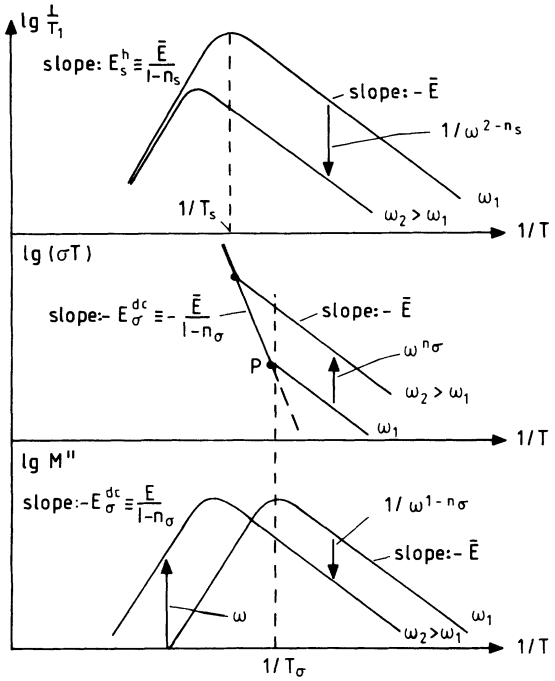

FIG. 1. Arrhenius representation (a) of ionic motion-induced SLR rate $1/T_1$, (b) of ionic conductivity σT, and (c) of dielectric modulus M'' as given by Eqs. (11)–(13) for two different frequencies ω_1, ω_2. Note that the SLR rate maximum occurs at a lower temperature T_s than the temperature T_σ of the maximum of M'' and the crossover point P of σT.

It will be shown that corresponding experimental data observed in a fluorozirconate glass can be interpreted by the model within some deviation indicating the limits of the simplified model.

II. THEORETICAL MODEL

Generally, the ion-induced SLR mechanism is caused by time-dependent fluctuations of the nuclear-spin coupling energy ω_{ij} between mutually interacting ion pairs (i,j).[11] The resulting SLR rate is determined by the Fourier transformation of the corresponding pair-pair correlation function

$$G_s(t)=\sum_{i,j}\langle\omega_{ij}(0)\omega_{ij}(t)\rangle_{\text{therm av}} . \tag{2}$$

Typically, the nuclear-spin coupling between the mobile ions is due to magnetic dipole or electric quadrupole interaction. Then, the coupling energy is given by $\omega_{i,j}\propto Y_{2,m}(\Omega_{ij})/r_{ij}^3$, where $Y_{2,m}$ denote the spherical harmonic and Ω_{ij} and r_{ij} are the spherical coordinates of the vector $\mathbf{r}_{ij}$ between the two ions (i,j) with respect to the direction of the external magnetic field B_0. It is worth noting that the $1/r_{ij}^3$ factor in ω_{ij} weights more heavily on the contribution to $G_s(t)$ from ion pairs at smaller separation. The SLR is related to wave vectors $k=k_0$ which are the inverse of the order of interatomic distances.[12]

On the other hand, ECR is related to the correlation function

$$G_\sigma(t)=\frac{q^2}{kT}\sum_{i,j}\langle\mathbf{v}_i(t)\cdot\mathbf{v}_j(0)\rangle_{\text{therm av}} , \tag{3}$$

where $\mathbf{v}_i(t)$ denote the velocities of the ions. The complex conductivity is given by the Fourier transformation of $G_\sigma(t)$. Obviously $G_\sigma(t)$ is a particle-particle correlation function which should be contrasted with $G_s(t)$, a pair-pair correlation function that emphasizes the contribution from ion pairs at close separations. Though the underlying process of ion diffusion is the same, in principle, the two correlation functions are different, i.e., SLR and ECR probe the ionic motion in a different manner. However, very recently Meyer, Maass, and Bunde[7,13] have shown that both correlation functions can be expressed in first approximation by stretched exponential functions in the relevant time regime ($10^{-3}\lesssim t/\tau_q\lesssim 10$), i.e.,

$$G_q(t)=\exp\{-(t/\tau_q)^{1-n_q}\} , \tag{4}$$

where $q\equiv\sigma$ for ECR and $q\equiv s$ for SLR, respectively. For that, they have studied by Monte Carlo simulation the thermally activated hopping motion of charged particles in a disordered lattice. Because of the Coulomb interaction a "slowing down" of the particle motion occurs for longer times (i.e., $t>t_c\simeq 10^{-11}$–10^{-12} s, where $t_c=1/\omega_c$ denotes the characteristic time of the slowing-down process) which is reflected by an exponent $1-n_q<1$, i.e., $n_q>0$. Switching off the Coulomb interaction leads to $n_q=0$ at intermediate times, i.e., to the common exponential decay of $G_q(t)$. Further, the authors have shown that the deviation between the two correlation functions $G_\sigma(t)$ and $G_s(t)$ is given by two different coefficients n_s and n_σ with $n_s>n_\sigma$ and two thermally activated correlation times τ_s and τ_σ exhibiting different preexponential factors as well as different activation energies. The relation $n_s>n_\sigma$ was confirmed experimentally in fast ion-conducting chalcogenide glasses by Borsa *et al.*[14]

According to the coupling model[8–10] the correlation times τ_q in Eq. (4) are linked to the individual ionic jump rate

$$1/\tau_0=(1/\tau_{0,\infty})\exp\{-\bar{E}/kT\} \tag{5}$$

for times $t>\omega_c^{-1}\simeq 10^{-11}$–$10^{-12}$ s as follows:

$$\tau_q=\{(1-n_q)\omega_c^{n_q}\tau_0\}^{1/(1-n_q)} . \tag{6}$$

Here, $\bar{E}$ denotes the microscopic barrier as seen by the hopping ion, ω_c is a cutoff frequency of the order of 10^{11}–10^{12} s^{-1} describing the high-frequency limit of ionic conductivity, and n_q has the same meaning as in Eq. (4).

Combining Eqs. (5) and (6) and taking into account that the exponents n_q are different for SLR and ECR ($n_s>n_\sigma$), one obtains immediately the following relations for the correlation times τ_q:

$$\tau_\sigma=\tau_{\sigma,\infty}\exp\{E_\sigma^{\text{dc}}/kT\} \tag{7}$$

with $E_\sigma^{\text{dc}}\equiv\bar{E}/(1-n_\sigma)$ and

$$\tau_s=\tau_{s,\infty}\exp\{E_s^h/kT\} \tag{8}$$

with $E_s^h \equiv \bar{E}/(1-n_s)$. The ratio of the preexponentials is given by

$$\frac{\tau_{s,\infty}}{\tau_{\sigma,\infty}} = \frac{[(1-n_s)\omega_c^{n_s}\tau_{0,\infty}]^{1/(1-n_s)}}{[(1-n_\sigma)\omega_c^{n_\sigma}\tau_{0,\infty}]^{1/(1-n_\sigma)}} . \quad (9)$$

Generally, from $n_s > n_\sigma$ it follows $\tau_{s,\infty}/\tau_{\sigma,\infty} \ll 1$. For instance, using $n_s = 0.75$, $n_\sigma = 0.6$, $\omega_c = 10^{12}$ s^{-1}, and $\tau_{0,\infty} = 10^{-13}$ s typical for ionic-conducting glasses one obtains $\tau_{s,\infty}/\tau_{\sigma,\infty} \simeq 10^{-3}$ in accord with experimental observations [see Eqs. (15) and (16) in Sec. IV and Ref. 5]. Furthermore, according to Eqs. (7) and (8) the coupling model relates the barrier height $\bar{E}$ to the energies E_σ^{dc} and E_s^h as follows:

$$\bar{E} = E_s^h(1-n_s) = E_\sigma^{dc}(1-n_\sigma) , \quad (10)$$

which provides more complete information than given by Eq. (1). In particular, $E_s^h = [(1-n_\sigma)/(1-n_s)]E_\sigma^{dc} > E_\sigma^{dc}$ for $n_s > n_\sigma$.

In order to calculate the SLR rate $1/T_1$ or the complex electric modulus M^* from the correlation function $G_q(t)$ given by Eq. (4), one has to go into the frequency domain by Fourier transformation (for details see Ref. 15). As pointed out, for instance, by Moynihan, Boesch, and Laberge[16] this cannot be performed analytically for an arbitrary exponent $1-n$ but has to be carried out numerically by expanding $G_q(t)$ in a power series. However, in a first approximation the dependence of the experimental observables on frequency ω and on correlation time τ_q can be expressed as follows:[12,17]

(i) SLR rate,

$$\frac{1}{T_1} \propto \frac{\tau_s}{1+(\omega\tau_s)^{2-n_s}} , \quad (11)$$

(ii) conductivity,

$$\sigma T \propto \frac{1}{\tau_\sigma}[1+(\omega\tau_\sigma)^{n_\sigma}] , \quad (12)$$

(iii) imaginary part M'' of the complex electric modulus,

$$M'' \propto \frac{\omega\tau_\sigma}{1+(\omega\tau_\sigma)^{2-n_\sigma}} . \quad (13)$$

It is important to note at this point that the interpretation of the experimental results in the present paper is based on Eqs. (11)–(13) using the coupling model to express the corresponding correlation times τ_s and τ_σ.

In order to have an overview of the main features a schematic sketch of the three observables $1/T_1$, (σT), and M'' is drawn in Fig. 1 in an Arrhenius representation for two different frequencies ω_1 and $\omega_2 (> \omega_1)$. The scheme offers the following experimental evaluations in order to determine the different properties describing the ionic jump process in glasses.

(a) The magnitude of the microscopic barrier, $\bar{E}$, can be determined from the slope of all three variables $1/T_1$, M'', and (σT) observed for $\omega\tau_q > 1$, i.e., at low temperatures.

(b) The temperature dependence of the correlation times $\tau_q = \tau_q(T)$ can be obtained from the position of the maxima of $1/T_1$ and M'' by means of the condition

$$\omega\tau_q(T_q) = [1/(1-n_q)]^{1/(2-n_q)} \simeq 2 \quad (n_q \simeq 0.6) \quad (14)$$

when varying the frequency ω in the experiments. As depicted in Fig. 1, it should be pointed out that generally the maximum of M'' and the corresponding crossover point P of (σT) occur at a lower temperature T_σ than the temperature of the maximum of $1/T_1$ observed at the same frequency because $\tau_s > \tau_\sigma$ in the relevant temperature range.

(c) Moreover, the corresponding activation energies E_s^h and E_σ^{dc} of the correlation times τ_q can also be determined from the Arrhenius representation of all three observables $1/T_1$, (σT), and M'' by measuring the slopes at high temperatures, i.e., for $\omega\tau_q < 1$. From $\bar{E}$, E_s^h, and E_σ^{dc} the parameters n_σ and n_s can be calculated by means of Eq. (10).

(d) The parameters n_σ and n_s are obtained also from the frequency dependence of the experimental data measured at low temperatures ($\omega\tau_q > 1$) as sketched in Fig. 1.

In the following we will show that the results of SLR and ECR experiments observed in slow ion-conducting fluorozirconate glasses can be explained consistently in the framework of relations given above demonstrating the capability of the approach. We should remind the reader, however, that the approach is based on the following three simplifying assumptions: (i) The correlation functions of various dynamical variables (q) originating from the same ionic jump process are presented by Eq. (4). (ii) The corresponding SLR and ECR observables are approximated by Eqs. (11)–(13). (iii) The coupling model relates the correlation times τ_q appearing in SLR and ECR by means of Eqs. (5) and (6) assuming an Arrhenius behavior for the individual uncorrelated ionic jump rate $1/\tau_0$ [Eq. (5)], i.e., a nearly constant barrier height $\bar{E}$. Monte Carlo simulations of Meyer, Maass, and Bunde[7] show that the correlation functions can be approximated by Eq. (4) but only in a limited time regime. Further, experimentally n_σ is not exactly constant[9,26] as assumed here. Also within the limitations and approximations of Monte Carlo simulations n_σ is expected to decrease with rising temperature but n_s should remain constant in the entire temperature region.

III. EXPERIMENT

The experiments were performed on fluorozirconate glasses of the following composition (in mol %): 27.4 ZrF_4, 27.4 HfF_4, 19.8 BaF_2 3 LaF_3, 3.2 AlF_3, 20 NaF (ZBLAN glass; $T_g = 553$ K). It is well known that F^- ions are responsible for the ionic conduction in these glasses.[3] The ^{19}F SLR rates have been measured at different Larmor frequencies by means of an upgraded Bruker SXP 4-100 pulse NMR spectrometer including a data acquisition system. The measurements were performed beginning at room temperature and rising the temperature up to about T_g. For each run an individual sample was used. Technical details of the high-

temperature NMR device are given elsewhere.[18,19] The conductivity measurements were carried out on the same samples using a Schlumberger Sl-1260 impedance meter and an electrometer-type preamplifier (Chelsea Dielectric) operating between 10 μHz and 10 MHz. Automatic control of the system and on-line data acquisition were performed by a computer.

IV. RESULTS AND DISCUSSION

According to Eqs. (11)–(13) the results of ECR experiments [conductivity (σT) and dielectric modulus M''] and SLR experiments (SLR rate $1/T_1$ in the laboratory frame and $1/T_{1\rho}$ in the rotating frame) presented in this section are based on contributions from diffusion of ions alone. In ionic glasses, however, at lower temperatures (or higher frequencies) there always exists an additional contribution to these measurable quantities from another mechanism. Although the exact nature of this mechanism is not well established at the moment, there is sufficient experimental evidence to suggest that it corresponds to relaxations of asymmetric double-well potential configurations (ADWP) with a distribution of energy barriers.[20,24,27] Thermally activated transitions between the two levels with a broad distribution of relaxation times give rise to a dielectric loss that is weakly frequency dependent and has a mild temperature dependence.[20–22] Such a dielectric loss corresponds to an excess ac conductivity, $\sigma_{ex}(\omega)$, which is nearly independent of temperature and shows an approximately $\omega^{1.0}$ dependence.[23] By the fluctuation-dissipation theorem, this excess conductivity corresponds to an excess $1/T_1|_{ex}$ or $1/T_{1\rho}|_{ex}$, which has an approximate T/ω dependence.[24] When compared with the ion diffusion this excess contribution becomes more important at lower temperatures and higher frequencies. Consequently, at sufficiently low temperatures and/or high frequencies, the measured ac conductivity may no longer be $\omega^{n_\sigma}\exp(-\bar{E}/kT)$ but instead has the excess conductivity form $\omega^{\delta}B(T)$, where $\delta \simeq 1.0$ and $B(T)$ has a very mild T dependence.[24,28] Similarly, the measured total $1/T_1|_t$ or $1/T_{1\rho}|_t$ at sufficiently low temperatures and high frequencies will not reflect the $\omega^{(2-n_s)}\exp(\bar{E}/kT)$ dependence but has instead an $\omega^{-\delta}C(T)$ dependence where $C(T)$ is another slowly varying function of T. In nonsuperionic conductors the ion diffusion contribution to ac conductivity and $1/T_1|_t$ is not large. It may dominate in the high-temperature and low-frequency regimes defined by $\omega\tau_\sigma \leq 1$ or $\omega\tau_s \leq 1$. However, it will certainly be overtaken by the excess ADWP contribution in the regimes $\omega\tau_\sigma \gg 1$ or $\omega\tau_s \gg 1$. In the transition zone between the two regimes, given by $\omega\tau_\sigma \leq 1$ and $\omega\tau_s \gg 1$, $1/T_1|_t$ in alkali oxide glasses is observed to have dependences of $1/T_1|_t \propto \omega^{-\delta}\exp(-\bar{E}/kT)$, where δ again is about 1.0. We have interpreted this as spin relaxation by transitions of ADWP assisted by a single alkali ion hop.[1,10] This transition zone is prominent in alkali oxide glasses (see Fig. 3 of Ref. 24) where $1/T_1|_t$ rises Arrheniusly more than 1 order of magnitude and $\bar{E}$ can unambiguously be determined.[1] This value of $\bar{E}$ from SLR together with E_σ^{dc} and n_σ obtained from ECR data verifies the relation $(1-n_\sigma)E_\sigma^{dc}=\bar{E}$ for many alkali oxide glasses.

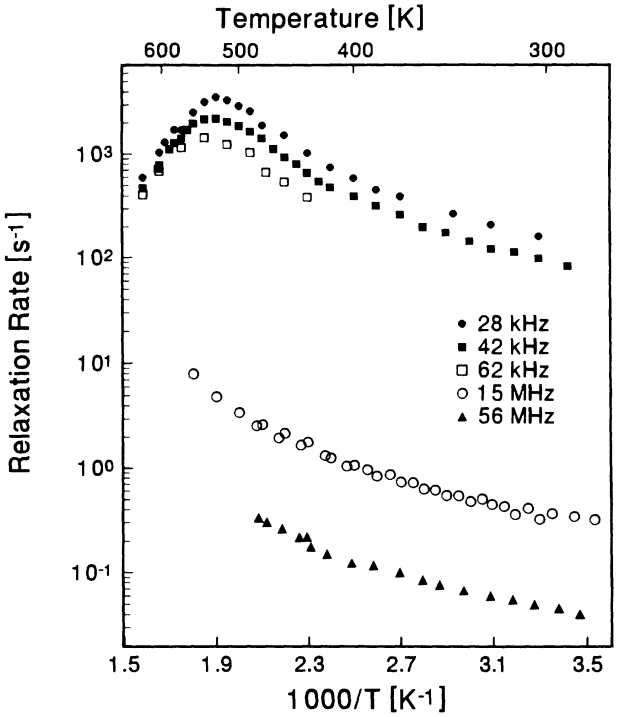

FIG. 2. Arrhenius plot of observed total ^{19}F SLR rates in the laboratory frame, $1/T_1|_t$, and in the rotating frame, $1/T_1\rho|_t$, measured in ZBLAN at different Larmor frequencies.

In comparison to oxide glasses, for fluorozirconate glasses, the transition zone involves no more than half a decade of $1/T_1|_t$ because of the low glass transition temperature T_g (see SLR data in Fig. 2). Obviously, in such a case the determination of $\bar{E}$ becomes difficult. In Refs. 2 and 3, the procedure of subtracting the excess $1/T_1|_{ex}$ or $1/T_{1\rho}|_{ex}$ contribution from the total measured values was used. This excess contribution which is about 10^{-1} s^{-1} at 100 K for ^{19}F under 15 MHz in ZBLAN was extrapolated within some error to higher temperatures. The resulting ionic motion-induced $1/T_1$ was fitted to an Arrhenius T dependence. The activation energy thus determined may underestimate the actual $\bar{E}$. Any incomplete subtraction of the ADWP-induced excess contribution from measured $1/T_1|_t$ or $1/T_{1\rho}|_t$ at low temperatures will yield a lower value for the actual $\bar{E}$. An alternative way to estimate $\bar{E}$ is to calculate the highest apparent activation energy for $1/T_{1\rho}$ on the low-temperature side of the observed maximum from $1/T_1|_t$ and $1/T_{1\rho}|_t$ data without subtracting off the excess contribution. This was performed in the present study for the SLR rate exhibited in Fig. 2. As listed in Table I within a relatively large uncertainty of 0.05 eV we found $\bar{E}=0.34$ eV. Further the frequency dependence of the SLR rates due to the low-temperature side of the maximum leads to a value of about 0.75 for the coefficient n_s. It should be noted that the observed very weak frequency dependence of the SLR rates at high temperatures was neglected in accord with the present model [Eq. (11)].

In exactly the same manner as we have just discussed

TABLE I. Summary of the parameters obtained from different evaluations of SLR and ECR data as discussed in the text.

	$\bar{E}$	Energies for $\omega\tau_Q < 1$ (eV)	n_q
SLR	0.33±0.05	E_s^h	0.7±0.15 [from energies, Eq. (10)]
		1.15 (from τ_s)	
		1.1 (from slope in Fig. 2)	0.75±0.07 (from freq. dependence)
ECR	0.35±0.04	E_σ^{dc}	0.54±0.05 [from energies, Eq. (10)]
		0.78 (from τ_σ)	
		0.85 (from slopes in Figs. 3 and 4)	0.59 (from freq. dependence)

for SLR, the excess ADWP contribution to ECR may tend to obscure the relation $(1-n_\sigma)E_\sigma^{dc}=\bar{E}$ expected for ion diffusion contribution [see Eq. (9)]. Figures 3 and 4 show the corresponding ECR data σT and M'' in an Arrhenius representation. Evaluation of the slopes of the curves in Fig. 3 leads to $E_\sigma^{dc}=0.87$ eV and $\bar{E}=0.37$ eV, while the corresponding slopes of Fig. 4 are given by $E_\sigma^{dc}=0.85$ eV and $\bar{E}=0.36$ eV. Pradel and Ribes have performed a similar evaluation of ECR and SLR (T_1) data in fast ionic-conducting chalcogenide glasses.[25] Further, the frequency dependence of the ECR data yields a value of 0.59 for the parameter n_σ of Eq. (4). The most important difference between SLR and ECR data of ZBLAN is manifested in their correlation times τ_s and τ_σ. As discussed before, τ_s is about an order of magnitude longer than τ_σ. This is confirmed by the more detailed analysis of electric modulus data in Fig. 4 which give directly τ_σ as a function of temperature. The result is presented in Fig. 5 leading to the following relation for τ_σ:

$$\tau_\sigma = 4.1\times10^{-15}\exp\left[\frac{0.78\text{ eV}}{kT}\right]\text{ s}. \tag{15}$$

Within a large error due to the limited frequency range of the observed SLR rates $1/T_{1\rho}$ (see Fig. 2), one is able to determine also the SLR correlation time τ_s from the maximum condition given by Eq. (14). We find

$$\tau_s = 6.6\times10^{-17}\exp\left[\frac{1.15\text{ eV}}{kT}\right]\text{ s}. \tag{16}$$

The corresponding line is depicted in Fig. 5, too. As

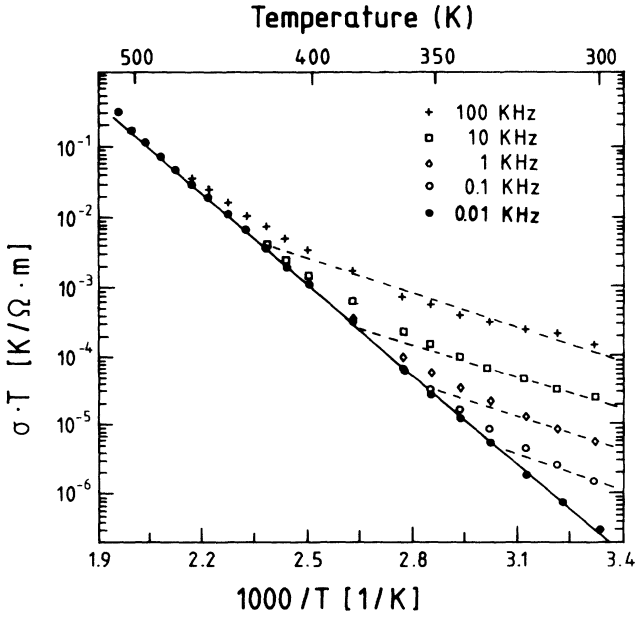

FIG. 3. Arrhenius plot of ionic conductivity (σT) in the same ZBLAN glass as in Fig. 2 measured at different frequencies. The lines are a guide to the eyes.

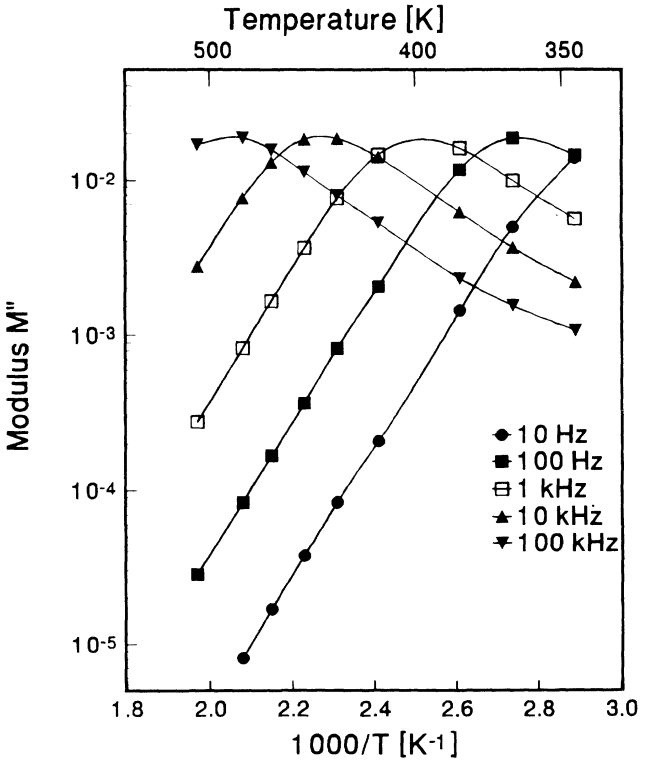

FIG. 4. Arrhenius plot of dielectric modulus M'' in the same glass as in Fig. 2 observed at different frequencies. The lines are a guide to the eyes.

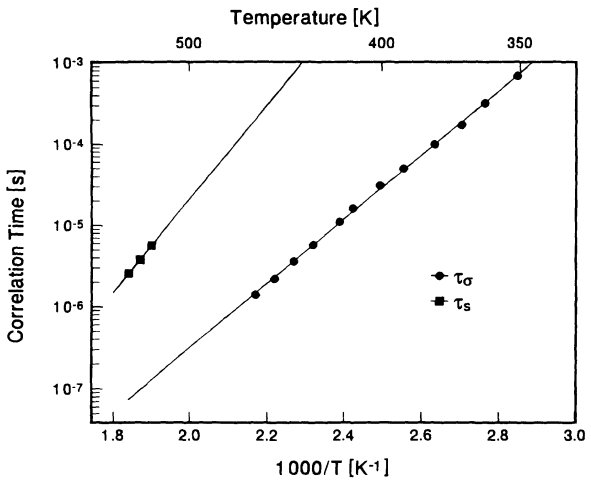

FIG. 5. Temperature dependence of the correlation times τ_σ from data analysis of M'' and of τ_s from frequency dependence of $1/T_{1\rho}$ maxima in Fig. 3.

can be seen from the figure in the relevant temperature regime between about 300 and 500 K, τ_s is significantly larger than τ_σ in accord with earlier observations. These data explain clearly the origin of the difference between the crossover temperature T_σ for conductivity and the temperature T_s of the SLR rate maximum, observed at the same frequency (see Fig. 1). For illustration, an example is shown in Fig. 6 exhibiting the ionic motion-induced SLR rate $1/T_{1\rho}$ obtained by optimized subtraction of the excess (ADWP) contribution from the observed SLR rate, $1/T_{1\rho}|_t$, and conductivity data (σT) taken at about the same frequency of 25 kHz. The data yield $T_s \simeq 525$ K and $T_\sigma \simeq 425$ K in agreement with the corresponding temperatures of 525 K for T_s and 425 K for T_σ determined from Fig. 5 using

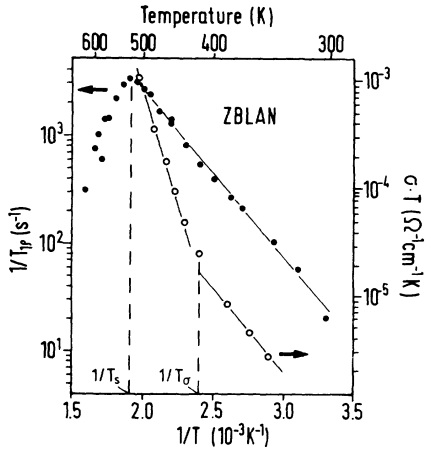

FIG. 6. Comparison of the temperature dependence of the ionic motion-induced part of the ^{19}F SLR rate, $1/T_{1\rho}$, and of ionic conductivity (σT) for ZBLAN, observed at the same frequency of about 25 kHz. Note the different temperatures T_s and T_σ of the SLR maximum and of the crossover point σT (see text).

$\tau = 1/2\pi\nu = 6.4 \times 10^{-6}$ s corresponding to 25 kHz.

The experimentally obtained activation energies E and parameters n governing the correlation functions [Eq. (4)] are summarized in Table I. In particular, the following set of parameters from Table I provides the best agreement with the main predictions of the model in terms of Eq. (10): $\bar{E} = 0.35$ eV, $E_s^h = 1.15$ eV, $E_\sigma^{dc} = 0.8$ eV, $n_s = 0.7$, and $n_\sigma = 0.56$. Further, using $\omega_c = 10^{12}$ s^{-1} and $\tau_{0,\infty} = 2 \times 10^{-13}$ s,[14,15] we estimate the preexponential times from Eqs. (5)–(8) as follows: $\tau_{s,\infty} \simeq 8 \times 10^{-17}$ s and $\tau_{\sigma,\infty} \simeq 4 \times 10^{-15}$ s. The values are in good accord with the experimentally observed data presented in Eqs. (15) and (16) indicating again the validity of relation (6) of the coupling model. One has to note again, however, that although the present model is able to interpret and relate the experimental SLR and ECR results there are some limitations. For instance, the two values for E_σ^{dc} listed in Table I which were determined with a high degree of accuracy show a noticeable difference which cannot be explained by the present model alone. Further, the parameter n_σ calculated numerically from Fourier transformation of $M''(\omega, T)$ was found to decrease weakly with rising temperature in accord with the results of Monte Carlo simulations by Meyer *et al.*[7] On the other hand, as pointed out by Nowick and co-workers[28,29] an alternative evaluation of conductivity data by means of Eq. (12) seems to lead to a temperature-independent value for n_σ at elevated temperatures. The finding would indicate that the exact correlation function $G_\sigma(t)$ may differ from Eq. (4).

V. SUMMARY

In this work we have revisited and analyzed SLR and ECR data of ZBLAN nonsuperionic glass to show the pronounced difference between the SLR time τ_s and the ECR time τ_σ. This corroborates the more recent findings by Tatsumisago, Angell, and Martin in superionic glasses.[5] An explanation of this pronounced difference is given in the framework of the coupling model. The key result is the inequality $n_s > n_\sigma$ between the coupling parameters of SLR and ECR, which is supported by a recent Monte Carlo simulation of SLR in a Coulomb lattice-gas model by Meyer, Maass, and Bunde.[7] Based on this result, the consequences of the coupling model are exploited to provide a detailed analysis of the ZBLAN experimental data. Various relaxation parameters continue to be related even though they are different for SLR and ECR, e.g., $n_s > n_\sigma$, $\tau_s \gg \tau_\sigma$, and $E_s^h > E_\sigma^{dc}$. This newly discovered drastic difference between SLR and ECR in superionic conductors by Tatsumisago, Angell, and Martin[5] and in nonsuperionic conductors by us[2] provides an important experimental fact to test the veracity of theoretical models of ion motion in glassy ionics. We have conducted low-frequency $1/T_{1\rho}$ measurements to compare with ECR measurements. This is a necessity for nonsuperionic conductors but not as much for superionic conductors. It would be interesting to extend this technique to superionic conductors where we expect an even more dramatic difference between τ_s and τ_σ.

ACKNOWLEDGMENTS

We would like to thank Professor A. Bunde, Professor W. Dieterich, and Professor A. Nowick for stimulating discussions, and R. Bölter, M. Herzog, and Dr. S. Estalji for performing part of the experiments. K. L. Ngai, H. Jain, O. Kanert, and R. Küchler were supported in part by ONR Contract No. N0001493WX24011, DOE Grant No. DE-F602-90ER45419, and the Deutsche Forschungsgemeinschaft, respectively.

[1](a) G. Balzer-Jöllenbeck, O. Kanert, H. Jain, and K. L. Ngai, Phys. Rev. B **39**, 6071 (1989); (b) G. Balzer-Jöllenbeck, O. Kanert, and H. Jain (unpublished); (c) H. Jain, G. Balzer-Jöllenbeck, and O. Kanert, J. Am. Ceram. Soc. **68**, C24 (1985).

[2]O. Kanert, R. Küchler, S. Estalji, K. L. Ngai, and H. Jain, in *The Physics of Non-Crystalline Solids,* edited by L. D. Pye *et al.* (Taylor and Francis, London, 1992), p. 178.

[3]S. Estalji, R. Küchler, O. Kanert, R. Bölter, H. Jain, and K. L. Ngai, J. Phys. (Paris) Colloq. **2**, C2-159 (1992).

[4]H. Jain and O. Kanert in *Proceedings of the International Conference on Defects in Insulating Materials (ICDIM 92),* edited by O. Kanert and M. Spaeth (World Scientific, Singapore, 1993), Vol 1, p. 274.

[5]M. Tatsumisago, C. A. Angell, and S. W. Martin, J. Chem. Phys. **97**, 6968 (1992).

[6]B. Munro, M. Schrader, and P. Heitjans, Ber. Bunsenges. Phys. Chem. **96**, 1718 (1992).

[7]M. Meyer, P. Maass, and A. Bunde, Phys. Rev. Lett. **71**, 573 (1993).

[8]K. L. Ngai, Solid State Ion. **5**, 27 (1981); Comment Solid State Phys. **9**, 141 (1980).

[9]K. L. Ngai, R. W. Rendell, and H. Jain, Phys. Rev. B **30**, 2133 (1984).

[10]K. L. Ngai and O. Kanert, Solid State Ion. **53-56**, 936 (1992).

[11]A. Abragam, *The Principles of Nuclear Magnetism* (Clarendon, Oxford, 1962).

[12]W. Dieterich, Solid State Ion. **40-41**, 509 (1990).

[13]A. Bunde, P. Maass, and M. Meyer, in *Proceedings of the International Conference on Defects in Insulating Materials (ICDIM 92),* edited by O. Kanert and M. Spaeth (World Scientific, Singapore, 1993), Vol 1, p. 295.

[14]F. Borsa, D. R. Torgeson, S. W. Martin, and H. K. Patel, Phys. Rev. B **46**, 795 (1992).

[15]U. Strom, K. L. Ngai, and O. Kanert, J. Non-Cryst. Solids **131-133**, 1011 (1992).

[16]C. T. Moynihan, L. P. Boesch, and N. L. Laberge, Phys. Chem. Glass **14**, 123 (1973).

[17]W. T. Sobal, I. G. Cameron, M. M. Pintar, and R. Blinc, Phys. Rev. B **35** 7299 (1987).

[18]B. Günther and O. Kanert, Phys. Rev. B **31**, 20 (1985).

[19]H. Kolem, O. Kanert, H. Schulz, and B. Günther, J. Magn. Reson. **87**, 160 (1990).

[20]G. Balzer-Jöllenbeck, O. Kanert, J. Steinert, and H. Jain, Solid State Commun. **65**, 303 (1988).

[21]O. Kanert, J. Steinert, H. Jain, and K. L. Ngai, J. Non-Cryst. Solids **131-133**, 1001 (1991).

[22]O. Kanert, M. Kloke, R. Küchler, S. Rückstein, and H. Jain, Ber. Bunsenges. Phys. Chem. **95**, 1061 (1991).

[23]K. L. Ngai, U. Strom, and O. Kanert, Phys. Chem. Glasses **33**, 109 (1992).

[24]O. Kanert, R. Küchler, J. Dieckhöfer, X. Lu, and H. Jain, Phys. Rev. B **49**, 629 (1994).

[25]A. Pradel and M. Ribes, J. Non-Cryst. Solids **131-133**, 1063 (1991).

[26]H. Jain, J. Non-Cryst. Solids **131-133**, 961 (1991).

[27]P. Heitjans, W. Faber, and A. Schirmer, J. Non-Cryst. Solids **131-133**, 1053 (1991).

[28]W. K. Lee, J. F. Liu, and A. S. Nowick, Phys. Rev. Lett. **67**, 1559 (1991).

[29]B. L. Lim, A. V. Vaysleyb, and A. S. Nowick, Appl. Phys. A **56**, 8 (1993).